THE JOURNAL OF PHYSICAL CHEMISTRY B

Article

pubs.acs.org/JPCB

On the Effects of Temperature, Pressure, and Dissolved Salts on the Hydrogen-Bond Network of Water

N. Galamba*

Grupo de Física-Matemática da Universidade de Lisboa, Av. Prof. Gama Pinto 2, 1649-003 Lisboa, Portugal

ABSTRACT: We study the structure of water through molecular dynamics, specifically the compression/expansion of the hydrogen-bond (H-bond) network, with temperature and pressure, and in salt solutions of alkali chlorides and sodium halides, and relate the observed local spatial perturbations with the tetrahedrality and the average number and lifetime of water H-bonds. The effect of transient H-bonds and transient broken H-bonds on H-bond lifetimes is further investigated, and results are compared with depolarized Rayleigh scattering lifetimes for neat water. A significant electrostriction is observed in the first hydration shell of Li^+ and F^-, while larger ions cause a small expansion of the H-bond network of water instead. However, both alkali cations and halide anions induce a minor contraction of the H-bond network in the second hydration shell. Further, water in the second hydration shell of Li^+, Na^+, and K^+ is less tetrahedral than neat water, resembling water at high pressures, while the H-bond network in the respective hydration shell of halide anions resembles water at low temperatures. Nevertheless, neither ion induced H-bond contraction nor expansion can be exactly mapped onto P or T effects on the local structure of water. Even though the average number and lifetime of H-bonds in the ionic hydration shells of most ions are not very different from those found in neat water, Li^+ and F^- significantly increase the lifetime of water donor and acceptor H-bonds, respectively, in the first hydration shell. The non-monotonic increase of cation and anion mobility, with ionic size, observed experimentally, is interpreted in terms of the water local tetrahedrality around cations and anions.

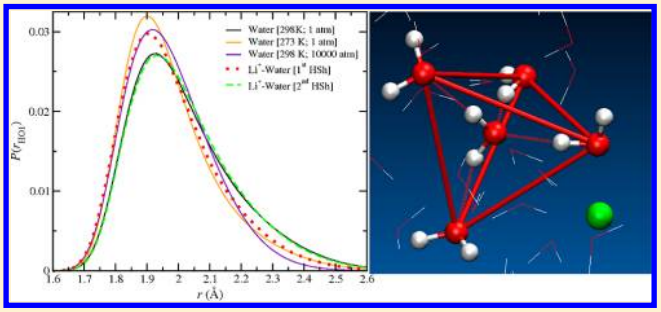

I. INTRODUCTION

Ions induce modifications on the structure and dynamics of water in the ionic hydration shells,[1−8] which in turn influence a number of processes in chemistry and biochemistry.[9−15] In spite of being intensively studied both experimentally[16−44] and theoretically,[45−81] ionic hydration and its implications in the water structure and dynamics remains a subject of ongoing debate. The hydration of both cations and anions is characterized by a negative enthalpy of hydration significantly lower than the associated negative entropy (i.e., $T\Delta S_{hyd}$), resulting in a negative Gibbs free energy of hydration.[82,83] The enthalpy of hydration of alkali cations and halide anions at room temperature increases (less negative)[82,84] from Li^+ to Cs^+ and from F^- to I^-, respectively, following the decrease of the charge density of the ions. Further, anions and cations with the same electronic configuration have different ionic radii and enthalpies and entropies of hydration, anions exhibiting a larger ΔS_{hyd} than cations. The entropy of hydration of an ion of charge z, $\Delta S_{hyd} = S(X^z, aq) - S(X^z, g)$, reflects the ionic "caging" by the surrounding water molecules in solution. Even though the ΔS_{hyd} of anions and cations can be understood to a large extent in terms of the strength of ion−water electrostatic interactions, especially for small ions, where excluded volume effects associated to cavity formation are less important,[85] a complete molecular-level comprehension of the reciprocal effects on the water structure and dynamics is complex and remains elusive. It is believed that the hydration of Li^+, F^-, and, to a minor extent, Na^+ lowers the entropy of water molecules in the ionic hydration shells, while the hydration of the other alkali cations and halide anions results in increased mobility and entropy of water.[20] Furthermore, dielectric friction and ion mobility should be closely related to these distinct ionic hydration atmospheres. The interpretation of several properties of salt solutions and biochemical processes involving ionic interactions is often undertaken with recourse to a distinction of ions in structure makers/breakers or kosmotropes/chaotropes, where the former are thought to reinforce the H-bond network of water and the latter to exert the opposite effect. Thus, small high charge density cations and anions are considered structure makers, while large cations and anions are structure breakers.[4] Ionic kosmotropes (Li^+, Na^+, and F^-) and chaotropes (K^+, Rb^+, Cs^+, Cl^-, Br^-, and I^-) are also often described as strongly and weakly hydrated ions,[15] respectively, independent of their hypothetical long-range effect on the H-bond network of water. This is similar to the concept of positive and negative hydration introduced by Samoilov,[8] which distinguishes ions that induce, respectively, longer and shorter water residence times, in the first ionic hydration shell, relative to bulk water. Further, the distinction of ions in kosmotropes and chaotropes is also often related to the position of the ions

Received: September 19, 2012
Revised: November 16, 2012
Published: December 23, 2012

in the Hofmeister[86] series, which orders anions and cations separately, according to their ability to salt out proteins. The suitability of a distinction of ions in structure makers/breakers has been questioned,[87] however, either because the H-bond network and the vibrational[34] and orientational dynamics[31,32] of water, beyond the first ionic hydration shell, are apparently similar to that of bulk water or because it does not account for local and long-range structural perturbations of water.[29,30,35] Neutron diffraction experiments, aided with the empirical potential structure refinement (EPSR) method, provided evidence that the effect of cations like Na^+ and K^+ in the structure of water is long-ranged[29,30] and that a distinction of ions in structure makers/breakers is misleading, since some ions, like Na^+, can tightly coordinate to water in the first hydration shell and disrupt the water structure outside the first hydration shell. Femtosecond mid-infrared (fs-IR) spectroscopy[31,32] results indicate that the orientational dynamics of water outside the first ionic hydration layer is similar to that of pure water. A fs-IR and dielectric relaxation spectroscopy study,[36] however, provided evidence that some ions induce a slowdown of the orientational dynamics beyond the first hydration layer that depends on the identity of the counterion.[36] A Raman spectroscopy investigation,[34] aided by simulation results, has also provided evidence that changes on the O−H vibrational spectrum of water induced by potassium halides in water result from the ion's electric fields, rather than reflecting any significant structural perturbations, and that the strength and number of H-bonds of water is not significantly modified outside the first ionic hydration shell.

The effect of ions on the structure of water has also long been described as comparable to that of temperature or pressure.[4,28,53,55,58] The electric field of ions is thought to induce an effect, on adjacent water molecules, similar to that of a compression force, reducing the volume of water, or other solvents, relative to the volume of the bulk solvent.[83,88−93] This so-called electrostriction effect depends both on the ions and on the solvent, and it should influence the dynamics of the solvent molecules on the ionic solvation shell(s).[90] Nonetheless, the way electrostriction influences the structure of water or its extent is not clear, in particular, whether it is restricted to the first ionic solvation shell, and outside the first coordination sphere the water volume is similar to that of neat water. A recent molecular dynamics work[53] on sodium halide solutions at different concentrations showed that the tetrahedrality of water in the second hydration shell of Na^+ and of the halide anions is modified in opposite ways. Here we probe water compression on the ionic hydration shells and relate local spatial perturbations with the tetrahedrality and the number and lifetime of water H-bonds. The non-monotonic increase of ion mobility, with radius size, is also interpreted in terms of the observed structural perturbations in the ionic hydration shells. Further, we compare specific ion effects on the H-bond network of water with those of temperature and pressure.

II. METHODS

Molecular dynamics (MD) simulations of aqueous solutions of a single ion pair of XCl [X = Li, Na, K, Rb and Cs] and of NaY [Y = F, Cl, Br and I] and 256 water molecules, at 298.15 K and 1 atm, were carried out with the flexible and polarizable force field AMOEBA 04.[94,95] The AMOEBA buffered 14-7[96] van der Waals parameters and polarizabilities for water's O and H atoms and for the alkali cations and halide anions are given in Table 1. The combining rules for heterogeneous atom pairs

Table 1. AMOEBA Buffered 14-7 van der Waals Parameters[a] and Polarizabilities, α, for Water and for the Alkali Cations and Halide Anions

cations				anions			
	R (Å)	ε (kcal/mol)	α (Å^3)		R (Å)	ε (kcal/mol)	α (Å^3)
H	3.405	0.110	0.496	O	2.655	0.0135	0.837
Li^+	2.38	0.08	0.028	F^-	3.40	0.25	1.35
Na^+	3.02	0.26	0.12	Cl^-	4.13	0.34	4.00
K^+	3.71	0.35	0.78	Br^-	4.38	0.43	5.65
Rb^+	4.14	0.44	1.35	I^-	4.66	0.52	7.25
Cs^+	4.37	0.53	2.26				

[a] R is the minimum energy distance and ε is the potential well-depth in the buffered 14-7 potential; for the alkali cations and halide anions, R is the ionic diameter.

used in AMOEBA are the cubic rule for R and the harmonic mean of the harmonic and geometric means for the well-depth, ε, of the minimum of the van der Waals interaction.[95,96] The average concentration of the different solutions is ∼0.2 M. MD of pure water at different temperatures and 1 atm and at different pressures and 298.15 K were also performed. The MD were performed with the program Tinker 5.1.[97] The long-range electrostatic interactions were calculated with the Ewald summation. Nonbonded van der Waals interactions and the Ewald real space summation were truncated at $L/2$, where L is the average length of the cubic MD box after equilibration. A modified Beeman algorithm was used to integrate the equations of motion with a time-step of 0.5 fs. The systems were first equilibrated for 150 ps in the (N,V,T) isokinetic[98] environment. This was followed by a (N,P,T) simulation for 300 ps at the same temperature and 1 atm, using the thermostat and barostat of Berendsen.[98] For the lowest temperatures (<298 K), an additional 500 ps were performed at (N,P,T) conditions for equilibration purposes. The production was carried out for 1.0 ns through MD (N,P,T) for the salt solutions and 0.5 ns for neat water at different T and P. We have verified that longer simulations (1 ns) for neat water do not change the results. The compression/expansion of the H-bond network of water was probed through the calculation of local structural parameters that do not depend explicitly on the density, allowing a characterization of the local structure of water in different regions of both the inhomogeneous salt solutions and pure water. We calculated the average distance of each water oxygen atom to the four nearest oxygen atoms of neighbor waters, denoted here by r_{O4},

$$\langle r_{O4} \rangle = \left\langle \frac{1}{N} \sum_{i=1}^{N} \left(\frac{1}{4} \sum_{j=1}^{4} r_{ij} \right) \right\rangle \quad (1)$$

where r_{ij} is the O−O distance, N is the number of water molecules considered to characterize a specific region of the salt solutions or the total number of water molecules for pure water, and $\langle\rangle$ denotes a time average. Further, we calculated the average distance of each oxygen to the two nearest hydrogen atoms of neighbor waters, r_{OH2}, given by

$$\langle r_{OH2} \rangle = \left\langle \frac{1}{N} \sum_{i=1}^{N} \left(\frac{1}{2} \sum_{k=1}^{2} r_{ik} \right) \right\rangle \quad (2)$$

dx.doi.org/10.1021/jp309312q | J. Phys. Chem. B 2013, 117, 589−601

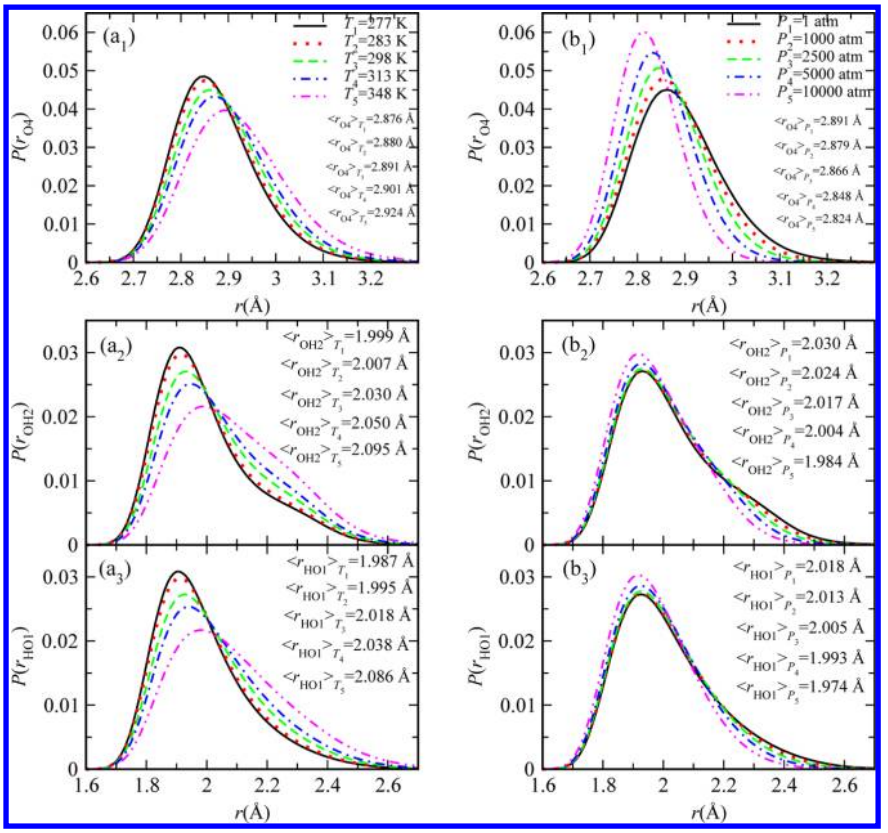

Figure 1. Local structure parameters, r_{O4}, r_{OH2}, and r_{HO1}, distribution, for neat water at different temperatures (a_1–a_3) and 1 atm and for different pressures (b_1–b_3) at 298.15 K. The respective average values are given in the plots. The long distance tails observed for $P(r_{HO1})$ and $P(r_{HO2})$ correspond to broken H-bonds.

where r_{ik} is the O–H distance. Finally, the distance of each hydrogen atom to the nearest oxygen atom of a neighbor water molecule was computed, r_{HO1},

$$\langle r_{HO1}\rangle = \left\langle \frac{1}{2N}\sum_{k=1}^{2N} r_{ki} \right\rangle \tag{3}$$

where r_{ki} is the H–O distance. The tetrahedrality of the H-bond network of water was probed with recourse to the orientational order parameter, q, proposed by Chau and Hardwick,[99] although in the rescaled version introduced by Errington and Debenedetti.[100] This parameter is given by

$$q = 1 - \frac{3}{8}\sum_{i=1}^{3}\sum_{j=i+1}^{4}\left(\cos\theta_{ij} + \frac{1}{3}\right)^2 \tag{4}$$

where θ_{ij} is the angle formed by the lines joining the O atom of a given water molecule and those of its nearest neighbors, i and j ($\leq$4); the average value of q varies between 0 (ideal gas) and 1 (perfect tetrahedral H-bond network). The number of water–water H-bonds was calculated using the following geometric criteria: $r_{OO} < 3.3$ Å and $\phi_{HOO} < 30°$, where r_{OO} is the distance between the donor and acceptor oxygen atoms and ϕ_{HOO} is the angle between the intramolecular O–H bond and r_{OO}. H-bond lifetime distribution functions[101] for water were calculated from

$$P(t) = \frac{N_{HB}(t, \Delta t)}{\sum_t N_{HB}(t, \Delta t)} \tag{5}$$

where $N_{HB}(t, \Delta t)$ is the number of donor or acceptor H-bonds that (i) remained unbroken at all times up to $t \pm \Delta t/2$ and (ii) got broken at $t \pm \Delta t/2$. $N_{HB}(t, \Delta t)$ was calculated through sampling of every time-origin, Δt was set to 2.5 fs, and the average H-bond lifetime, $\tau_{HB} = \int_0^\infty tP(t)\,dt$, was approximated by $\tau_{HB} = \sum_t tP(t)$. The water and ion self-diffusion coefficients were estimated through the Green–Kubo integral[102]

$$D = \frac{1}{3N}\int_0^\infty \langle \sum_{i=1}^{N} \mathbf{v}_i(0)\cdot\mathbf{v}_i(t)\rangle\, dt \tag{6}$$

and the ion mobilities, u_q, were computed from the Einstein relation, $u_q^{\pm} = D_{\pm}g_{\pm}/k_BT$, where $q_{\pm}$ is the ionic charge and k_B is the Boltzmann constant.

III. RESULTS AND DISCUSSION

The water molecules in a salt solution reorient differently around cations and anions, forming hydration shells where both H atoms point away from a cation and a single H atom points toward anions to form a water–anion H-bond. A water molecule in the first hydration shell of a cation is, therefore, free to form two donor H-bonds and accept a single H-bond, and in the first anionic hydration shell, water molecules can accept two H-bonds and form a single H-bond as proton donors. Thus, r_{HO1} was used to probe the water local structure in the first cationic hydration shell, r_{HO2} in the first anionic hydration shell, and r_{O4}, r_{OH2}, and r_{HO1} were used to probe the structure in the second and third ionic hydration layers. The same local structure parameters were also used to probe the structure of neat water at different temperatures and pressures.

Temperature and Pressure Effects. The effect of temperature and pressure on the local structure of water as probed by r_{O4}, r_{OH2}, and r_{HO1} is depicted in Figure 1. The

dx.doi.org/10.1021/jp309312q | J. Phys. Chem. B 2013, 117, 589–601

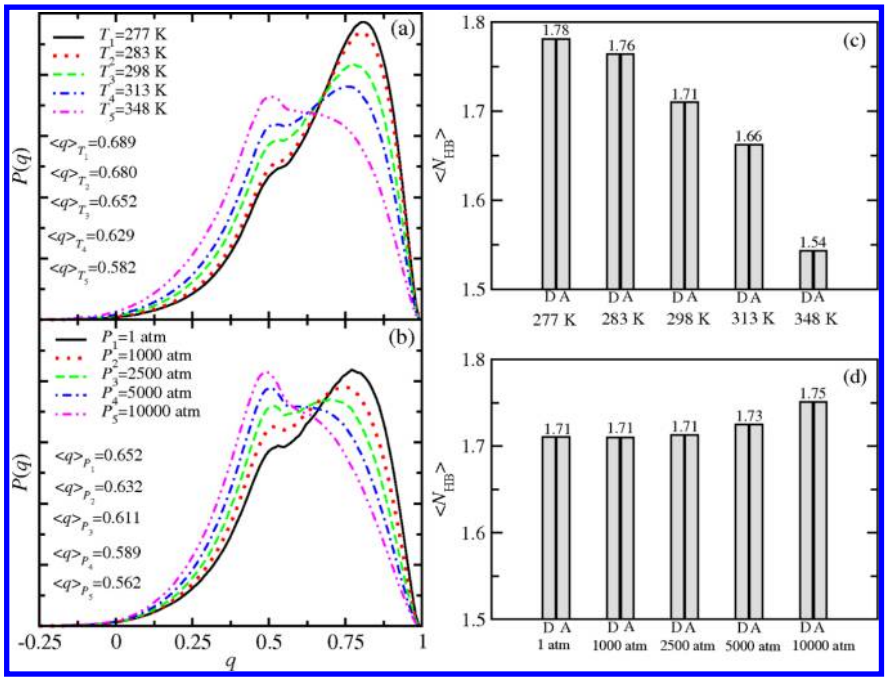

Figure 2. Distribution of the tetrahedral parameter q for neat water at (a) distinct temperatures and 1 atm and (b) at distinct pressures and at 298.15 K and the average number of donor (D) and acceptor (A) H-bonds at (c) different temperatures and (d) pressures. The respective average values are given in the plots.

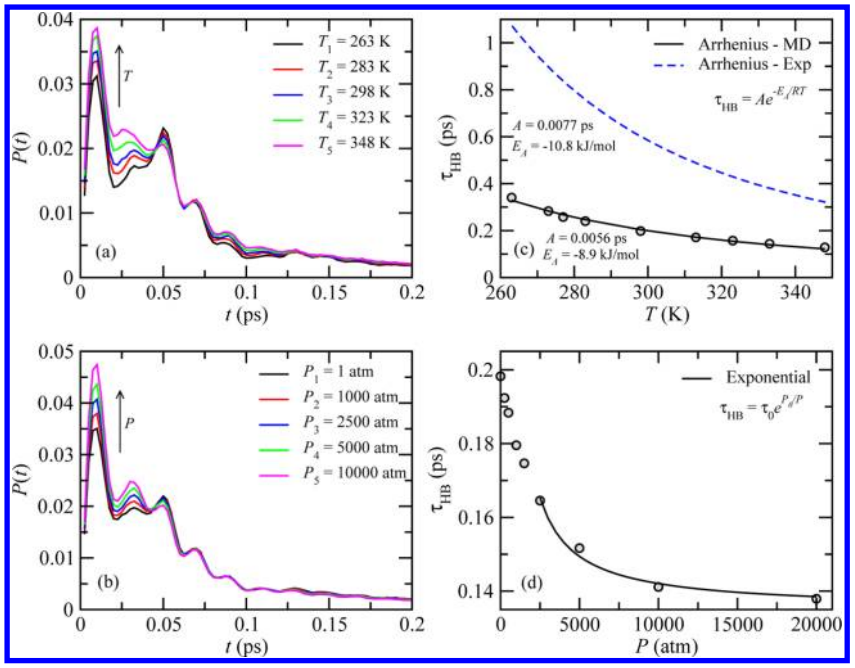

Figure 3. H-bond lifetime distributions in neat water at different (a) temperatures and (b) pressures and the respective average lifetimes, τ_{HB}. The long-time tail of $P(t)$ extends up to [22.8, 12.2, 10.1, 6.3, and 4.1 ps] from the lowest to the highest T and up to [10.1, 7.4, 6.9, 5.9, and 7.3 ps] from the lowest to the highest P. The Arrhenius curve fitted to depolarized light scattering experimental data of Conde and Teixeira[105] is shown in part c.

distributions $P(r_{O4})$, $P(r_{HO1})$, and $P(r_{OH2})$ provide information on the neighborhood of the O and H atoms of a water molecule, independent of the existence of H-bonds with its nearest neighbors. As it may be seen, the distributions are not normal; rather long distance tails are observed, in particular, for $P(r_{HO1})$ and $P(r_{OH2})$. These tails indicate the existence of broken H-bonds for distances larger than the first minimum of the water OH radial distribution function (rdf), 2.44 Å; the OH coordination number (CN) of AMOEBA water is 1.9. The fact that $P(r_{O4})$ does not extend in any significant way beyond 3.3 Å means that H-bond breaking is caused almost exclusively by librational movements, as expected. Even though the first minimum of the O−O rdf of AMOEBA water appears at ∼3.47 Å, we have, therefore, chosen a more restrictive distance definition, 3.3 Å; the CN at this distance is 4.5. The O and H atoms average distance to the nearest neighbors increases with temperature and decreases with pressure. Further, although both low T and high P originate a contraction of r_{O4}, r_{OH2}, and

dx.doi.org/10.1021/jp309312q | J. Phys. Chem. B 2013, 117, 589−601

r_{HO1}, these exhibit marked differences. In particular, pressure causes a significant shift of the peak of $P(r_{O4})$ to lower distances, while the peaks of $P(r_{HO1})$ and $P(r_{OH2})$ are nearly unchanged, and lower average values of r_{OH2} and r_{HO1} result from the contraction of the long distance tails. This suggests that the number of H-bonds at high pressures increases relative to water at 1 atm (see below). For water at low and high T, the distributions shift, respectively, to shorter and longer distances, relative to water at room temperature. It should be noted that lower average r_{O4}, r_{OH2}, and r_{HO1} do not necessarily signify that water is denser in that particular region; for instance, supercooled water has lower average r_{O4}, r_{OH2}, and r_{HO1} distances, "similar" to water at high P, in spite of a lower density relative to room T water; the reason is that supercooled water is highly tetrahedral, while pressure disrupts significantly the tetrahedral orientational order of water (see discussion below).

Figure 2 shows the bimodal distribution of the tetrahedral parameter, q, at different T and P. The peak at lower q associated to low tetrahedrality water is significantly enhanced with both the T and P increase, and at sufficiently large T or P, it becomes the main peak of $P(q)$. On the other hand, at low T, this peak shifts downward and at sufficiently low temperatures it nearly disappears. Thus, pressure cuts the distance of an oxygen atom to its four nearest O neighbors (see Figure 1), the latter diverging from the vertices of a regular tetrahedron, while water at low temperatures exhibits a distinct contraction effect, with the four nearest O neighbors arranged in a more ice-like tetrahedral geometry. Nevertheless, in spite of water's tetrahedrality disruption with P, the (average) number of H-bonds, N_{HB}, at room temperature is nearly pressure invariant (see Figure 2) up to 2500 atm. N_{HB} passes through an almost unnoticeable minimum around 250 atm (not shown here), and it slightly increases at large pressures (≥5000 atm) consistent with the observed contraction of the long distance tails of $P(r_{HO1})$ and $P(r_{OH2})$, noted before. Hence, for the geometric H-bond definition adopted here, pressure deforms H-bonds without significantly changing their average number, reflecting the remarkable ability of water to preserve its H-bond network. The average number of H-bonds of liquid water at 1 atm, on the other hand, decreases by less than 0.3 in passing from 277 to 348 K, although the tetrahedrality of water is significantly perturbed. The average H-bond lifetime, τ_{HB}, shown in Figure 3, in turn, decreases with the T and P increase. In particular, the fraction of H-bonds that break at sub-ps times (<0.05 ps) due to fast librational movements increases with T and P, and the fraction of long-lived H-bonds decreases. Interestingly, at large pressures (≥10 000 atm), a long time tail reappears, indicating the existence of a small subset of H-bonds that have longer lifetimes than at lower pressures. Thus, at 10 000 and 20 000 atm, we find maximum H-bond lifetimes of 7.3 and 10.7 ps, respectively. The latter is already larger than the maximum found at 1 atm, of 10.1 ps. Nonetheless, a much larger population of H-bonds have significantly lower lifetimes and therefore the average τ_{HB} decreases monotonically with pressure (Figure 3d); τ_{HB} decreases linearly with P, below 1500 atm, and a nearly exponential behavior is observed with $1/P$ at larger pressures. Regarding the temperature dependence, τ_{HB} exhibits an Arrhenius behavior, in agreement with both experiments[103−106] and MD simulations[101] of SPC/E water. The τ_{HB} for water at the melting temperature, 273 K, and supercooled water, 263 K, are also reported to probe a T interval similar to that of the experiments of Conde and Teixeira.[105] The activation energy E_A, interpreted as the energy required to break an H-bond through water librational motions,[104] is found to be 8.9 kJ/mol, ∼2 kJ/mol lower than that found from depolarized light scattering measurements,[101,103] 10.8 ± 1.0 kJ/mol. The E_A for AMOEBA water is, however, similar to the 8.8 ± 1.0 and 9.3 ± 1.0 kJ/mol activation energies found by Starr et al.[101,107] for SPC/E water using energetic and geometric H-bond definitions, respectively. The H-bond lifetime for AMOEBA water at 298.15 K, τ_{HB} = 0.20 ps, is also similar to that of SPC/E water[107] for the energetic H-bond definition, 0.18 ps, at 300 K, and lower than that obtained with the geometric definition, 0.27 ps. The experimental (Arrhenius equation fit) lifetimes from Conde and Teixeira[105] are significantly larger, namely, 0.62 and 0.60 ps for water at 298 and 300 K, respectively. Thus, in spite of the dependence of τ_{HB} on the H-bond definition, this discrepancy should have another origin. In particular, we can question if experimental relaxation times from depolarized spectra[105,106] are sensitive to (i) H-bonds that break and reform with the same partner after a small period of time ($<t^*$) due to small angle librations and (ii) transient ($\tau_{HB} < t^{**} = t^*$) H-bonds that form and break without later reforming within a similar time interval ($<t^*$). Neglect of this intermittence in the calculation of τ_{HB} in a MD could explain the relatively low lifetimes observed for AMOEBA and SPC/E water. This dependence was investigated here for both (i) transient broken H-bonds and (ii) transient H-bonds. The former were probed by recalculating H-bond lifetimes "excluding" transient broken H-bonds, that is, H-bonds that break and reform with the same partner within a tolerance time, t^*. Thus, if an H-bond between water molecules i (donor) and j (acceptor) breaks and reforms within t^*, the H-bond is considered unbroken during the tolerance time. A further restriction is imposed, namely, that during the tolerance time the proton of the water donor i does not form an H-bond with a third water acceptor k. The H-bond lifetimes reported here are therefore for donor water molecules and were computed for t^* = 0.1 ps; note that the H-bond lifetimes shown in Figure 3 correspond to t^* = 0 ps. The t^* = 0.1 ps corresponds approximately to the transient nonexponential part of the orientational autocorrelation function, $C_2(t)$, and concomitantly encompasses the peaks of the HB lifetime distribution (see Figure 3), corresponding to large populations of transient H-bonds. The orientational autocorrelation function, $C_2(t) = P_2[\mathbf{u}_{r_{OH}}(t)\cdot\mathbf{u}_{r_{OH}}(t + dt)]$, where $\mathbf{u}_{r_{OH}}$ is the intramolecular OH unit vector and P_2 is the second-order Legendre function, is depicted in the inset of Figure 4a for AMOEBA water at 298 K. The reorientation time of water obtained from the time integral of the orientational autocorrelation function is 2.17 ps, consistent with nuclear magnetic resonance experimental data, 1.7−2.6.[108] The H-bond lifetime distributions, $P(t)$, of water at 298 K for t^* = 0 ps and t^* = 0.1 ps are plotted in Figure 4. A significant decrease of the population of transient H-bonds can be observed, leading, in turn, to larger populations of longer lifetime H-bonds. Figure 4b shows the τ_{HB} for water at different T and the respective Arrhenius fitted curves. The effect of excluding transient broken H-bonds is larger at lower T, and the MD H-bond lifetimes are closer to the experimental lifetimes, although a significant discrepancy still exists. The pre-exponential factor and the E_A for t^* = 0.1 ps are 0.0062 ps and 9.7 kJ/mol, respectively, also closer to the experimental values. The $P(t)$ for t^{**} = 0.1 ps, shown in Figure 4a, was calculated by neglecting both transient

dx.doi.org/10.1021/jp309312q | J. Phys. Chem. B 2013, 117, 589−601

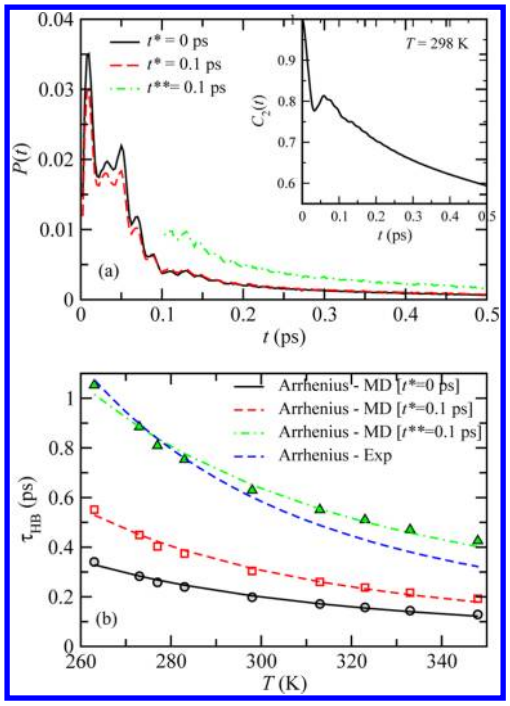

Figure 4. (a) Effect of transient broken H-bonds and transient H-bonds on the H-bond lifetime distribution for neat water at 298 K. The inset shows the first 0.5 ps of the orientational autocorrelation function of AMOEBA water. (b) MD and experimental H-bond lifetimes for neat water at different temperatures. The Arrhenius equation parameters $[A, E_A]$ for the tolerance time. $t^* = 0.1$ ps and $t^{**} = 0.1$ ps are, respectively, [0.0062 ps, 9.7 kJ/mol] and [0.023 ps, 8.3 kJ/mol].

($t^* = 0.1$ ps) broken H-bonds and transient H-bonds ($\tau_{HB} < t^{**} = 0.1$ ps), discussed above (ii). The corresponding lifetimes are plotted in Figure 4b. As it can be seen, when both transient broken H-bonds and transient H-bonds are neglected, the agreement with the experimental data is excellent at low temperatures and at $T \geq 298$ K the calculated τ_{HB} are significantly overestimated. The agreement of the pre-exponential factor, 0.023 ps, and E_A, 8.3 kJ/mol, is in fact worst because of the lifetimes at high temperatures. These results suggest, on the one hand, that depolarized Rayleigh scattering experiments are insensitive to transient broken H-bonds and transient H-bonds and, on the other, that the AMOEBA water dynamics is slower than real water, at room and higher temperatures. The latter is consistent with the fact that AMOEBA underestimates the self-diffusion coefficient of water at room T.[109] This was confirmed here, and $D = 1.9 \times 10^{-5}$ cm^2 s^{-1} was found from the Green−Kubo integral of water's center of mass velocity autocorrelation function, ∼17% lower than the experimental[110] value, $D = 2.3 \times 10^{-5}$ cm^2 s^{-1}.

Cation Specific Effects. The distinct parameters discussed here for a specific ionic hydration shell were calculated for those water molecules in that specific hydration shell and, concomitantly, not at a distance smaller than the third hydration shell minimum of the counterion. The distribution of r_{O4}, r_{OH2}, and r_{HO1} in the first, second, and third hydration shells of Li^+ to Cs^+ are displayed in Figure 5. As it may be seen, Li^+ induces a significant contraction of r_{HO1} in the first hydration shell. For Na^+ and K^+, a small expansion is observed instead, whereas for Rb^+ and, especially for Cs^+, an even smaller expansion takes place. The CNs of the cations found here are respectively 4.3, 5.7, 6.8, 7.6, and 8.9 for Li^+ to Cs^+ as obtained from integration of the X^+−O rdf up to the first minimum. These CNs are slightly larger than some of the values reported from neutron and X-ray scattering studies,[7,30,111−113] except for Li^+. The CN of Li^+ has long been the object of controversy, with experimental and simulation results predicting 4−6 nearest neighbors.[113−115] The CN obtained here is consistent with the theoretical *ab initio* results of Rempe et al.[115] Electrostriction of water on the first hydration shell of Li^+ is comparable to compressed water at $P > 5000$ atm, and below 10 000 atm, regarding the r_{OH1} distance. However, $P(r_{HO1})$ exhibits marked differences from the distributions for neat water at high P (and at low T; see Figure 6a). A small compression of water's H-bond network in the second hydration shell of the alkali cations can be observed, while the third hydration layer resembles already neat water, although for Li^+ and Cs^+ a very small compression and expansion, respectively, appears to occur. The fact that a significant compression is not observed in the second hydration shell of Li^+ shows that, although the contraction of the intermolecular H−O distance in the first hydration layer is very strong, electrostriction effects are short-ranged.

The tetrahedral parameter distributions plotted in Figure 7 show that, for Li^+, Na^+, and K^+, water in the second ionic hydration shell is less tetrahedral than neat water, while in the third hydration shell the effect is almost nonexistent. Thus, water in the second hydration shell of the alkali cations resembles water at high pressures. Nonetheless, the fact that the parameters, r_{O4}, r_{OH2}, and r_{HO1}, for any cation, cannot be exactly mapped onto those of water at high pressures further supports the view that pressure and electrostriction effects are not exactly equivalent. Notice that the tetrahedrality of water probed in the second ionic hydration shell depends on the orientation of water molecules in the first hydration shell. Thus, for water molecules at the innermost part of the second ionic hydration shell, the four vertex oxygen atoms are in the first and second ionic hydration shells. The most unexpected result found here is perhaps the expansion of water in the first ionic hydration shell of Na^+, similar to K^+. The sodium cation is believed to lower the entropy of water molecules in its vicinity,[20] and to increase the activation energy for water exchange between the first and second hydration shells,[8] although to a much lesser extent than Li^+ and F^-, and for this reason, Na^+ is often considered a weak kosmotrope. The behavior of Na^+ observed here appears to be consistent with recent X-ray Raman scattering spectroscopy results,[42] which suggest that Na^+ weakens water H-bonds in its vicinity. This weakening has been associated with high density, H-bond distorted (asymmetric), liquid (HDL) water.[42,116] Here we observe a significant disruption of the tetrahedrality of water around Na^+ (see Figure 7), comparable to that of water at 1000 atm, a small contraction of the H-bond network in the second hydration shell, and a larger r_{HO1} distance in the first hydration shell, comparable to water at 313 K. These results suggest therefore that weaker H-bonds are formed between water molecules in the first and second hydration shells of Na^+.

For Rb^+ and Cs^+, the effect on the tetrahedrality, if any, is too small, although interestingly, Cs^+ appears to induce a small tetrahedral enhancement of water. This suggests that volume exclusion effects associated to cavity formation contribute to the enhancement of orientational order of water, in agreement with the observation that I^- is the halide anion that induces the largest tetrahedrality enhancement of water among the halide anions.[53] A similar, although more pronounced effect has also

dx.doi.org/10.1021/jp309312q | J. Phys. Chem. B 2013, 117, 589−601

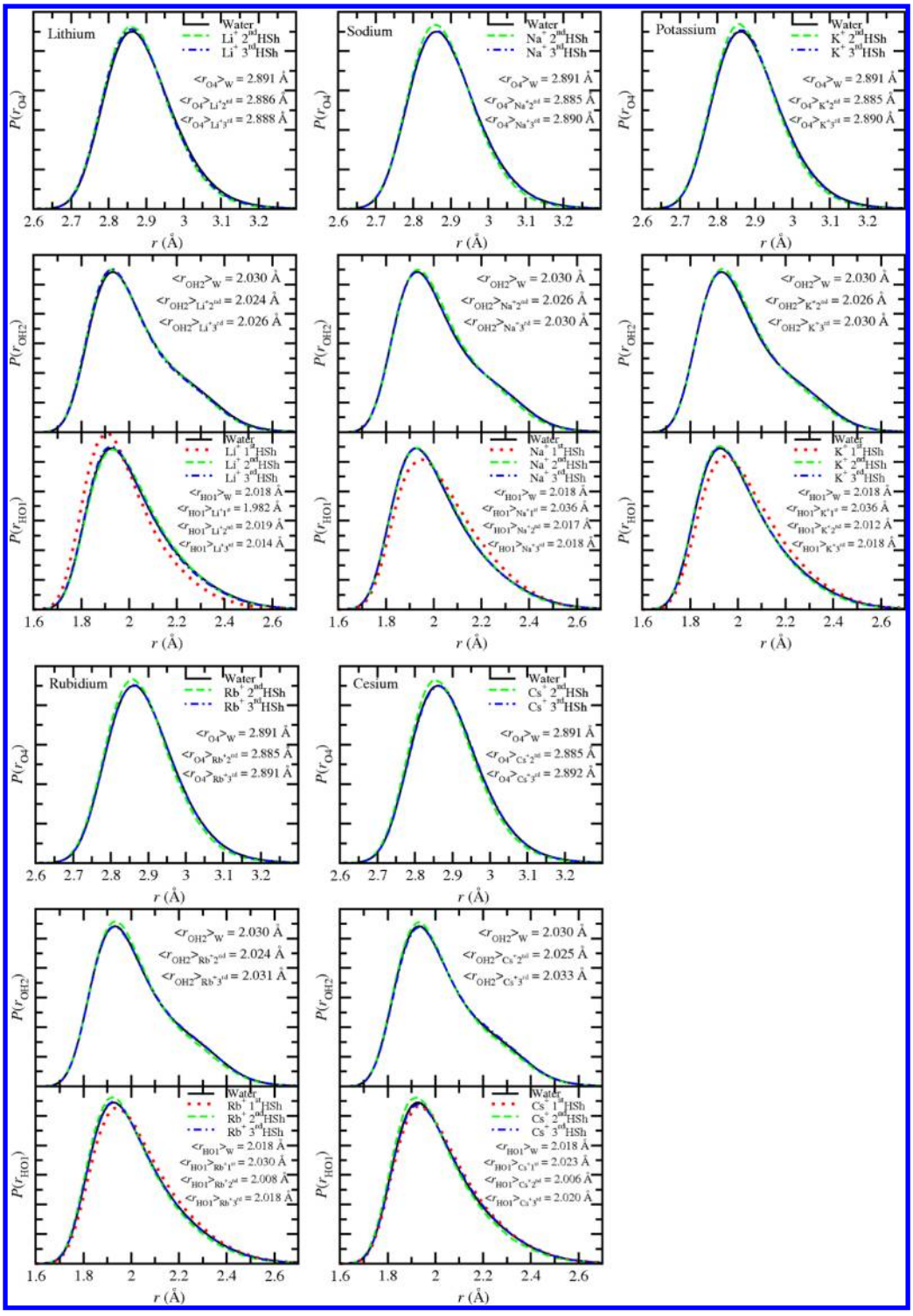

Figure 5. Structure parameters, r_{O4}, r_{OH2}, and r_{HO1}, distribution, for the first (r_{HO1}), second, and third hydration shells of the alkali cations. The respective average values are given in the plots.

been recently reported for benzene in water.[117] The number of water H-bonds in the cationic hydration shells, shown in Figure 8, is similar to that of neat water. Nevertheless, a small increase of donor HBs in the first hydration shell of Li^+ can be observed, in agreement with its structure maker reputation, and a slight reduction for the other alkali cations. The increase of acceptor H-bonds in the first hydration shell in passing from Li^+ to Cs^+, on the other hand, correlates well with weaker ion−water electrostatic interactions and the closely related increase of the CN. Notice that the height of the first minimum of the X^+−O rdf's (not shown here) also increases in this order, indicating lower residence times and therefore greater rotational and translational freedom, since passage from the first to the second hydration shells involves H-bond breaking.

We now discuss the water H-bond lifetimes in the cationic hydration shells; calculations are reported here for a tolerance time of $t^* = 0$ ps. The escape of water molecules with unbroken H-bonds from an ion's hydration shell was accounted for

dx.doi.org/10.1021/jp309312q | J. Phys. Chem. B 2013, 117, 589−601

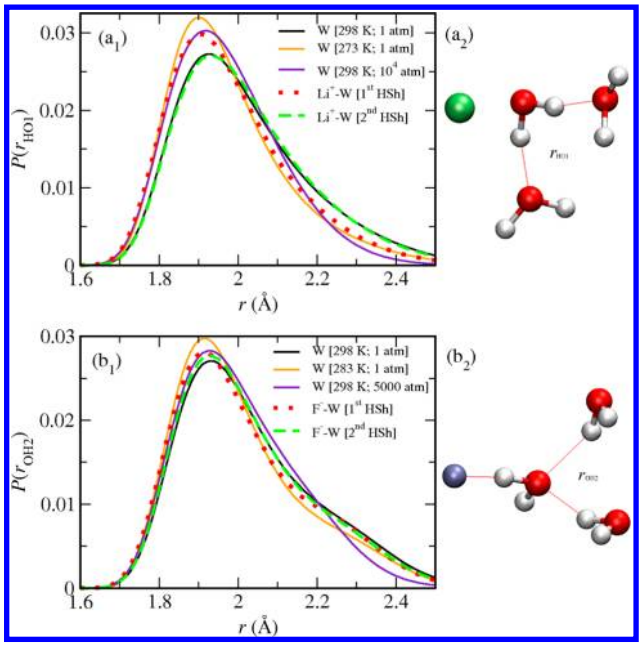

Figure 6. Effect of (a_1) Li^+ and (b_1) F^- compared to that of low T and high P on the local structure of water. Parts a_2 and b_2 illustrate the distances, r_{HO1} and r_{OH2}, for a water molecule in the first hydration shell of Li^+ and F^-, respectively; note that the respective nearest neighbors (O atoms for Li^+ and H atoms for F^-) in the second hydration shell and the water molecule in the first hydration shell (H atoms for Li^+ and O atom for F^-) are not necessarily H-bonded.

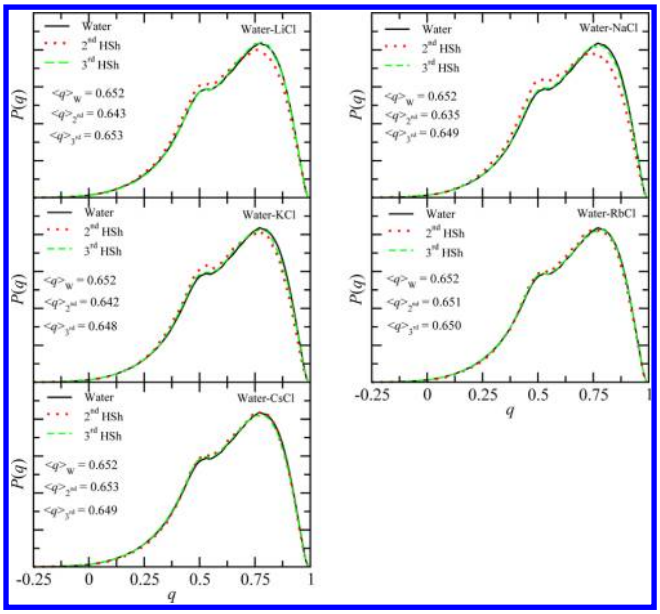

Figure 7. Distribution of the tetrahedral parameter q for neat water at 298.15 K and 1 atm and for the second and third hydration shells of the alkali cations. The respective average values are given in the plots.

through the following protocol, based on the residence time definition, of Impey et al.:[61] if a water molecule, i, H-bonded to a molecule j, leaves the hydration shell with the H-bond intact, its lifetime inside and outside the hydration shell is counted if the molecule returns to the hydration shell with the H-bond unbroken, after a period no longer than a defined digression time, t_d. If the molecule returns after t_d or the H-bond breaks, during the period the molecule is outside the hydration shell, the time interval outside the hydration shell is neglected. Notice that, although transition involves some H-bond breaking, water molecules can preserve probably at least one H-bond intact during passage. The relative population of unbroken H-bonds during hydration shell transitions is, nevertheless, very low, and therefore, we found the results to be almost independent of t_d, unlike residence times.[118] For instance, for the first hydration shell of Li^+, the average H-bond lifetimes of donors and acceptors for t_d equal to 0.2 and 2.0 ps are, respectively, (0.21 ps, 0.12 ps) and (0.21 ps, 0.12 ps); for Cs^+, which has a significantly lower residence time, these values are (0.16 ps, 0.15 ps) and (0.16 ps, 0.16 ps). The H-bond lifetimes of pure water in the self-hydration shells were also probed through this protocol to allow a direct comparison with the salt solutions. A single water molecule was defined as the solute and H-bond lifetimes were calculated for the first, second, and third hydration shells of water; H-bonds between water molecules in the first hydration shell and the "solute" water molecule were neglected. The average H-bond lifetimes in the hydration shells were computed for t_d = 2.0 ps and are given in Table 2. Li^+ is the only cation that induces longer donor τ_{HB} in the first hydration shell. A lower rotational freedom of water near Li^+, on the other hand, explains the small number and low τ_{HB} of acceptor H-bonds in the first ionic hydration shell, both of which increase in an ordered way in passing from Li^+ to Cs^+ (see Figure 8). Another difference between pressure and electrostriction concerns the H-bond lifetime; thus, contrary to water at high pressures, water donor H-bonds in the first hydration shell of Li^+ have longer lifetimes. Outside the first hydration shell, τ_{HB} is similar for all the cations and to neat water, indicating, therefore, that the effect of the cations on the orientational dynamics of water is relatively short-ranged, similar to compression and expansion of water's H-bonds.

Anion Specific Effects. We now consider anionic hydration in the sodium halide aqueous solutions. Figure 9 shows that, like for alkali cations, only the smallest anion, F^- (Na^+ iso-electronic), causes a compression of the H-bond network in the first hydration shell, although significantly lower than for Li^+, consistent with weaker ion−water electrostatic interactions and a lower enthalpy of hydration. However, like for Li^+, significant differences can be observed for $P(r_{OH2})$, relative to water at high P or low T (see Figure 6b). A small contraction of the H-bond network in the second hydration shell is also observed for the halide anions, *apparently* similar to that for alkali cations. The halide anions, however, enhance the tetrahedral orientational order of water in the second hydration shell at low concentrations,[53] in opposition to cations, and therefore anionic hydration resembles, in this sense, water at low T, rather than water at high P; at large concentrations, the dominant disruption effect of Na^+ cancels out[53] the tetrahedral enhancement in the anionic second hydration shell. X-ray absorption spectroscopy (XAS) results[43] for NaF and KF aqueous solutions foresee the existence of an increased fraction of tetrahedral low-density liquid (LDL) structures due to the presence of the F^- ions. However, it was unclear from interpretation of XAS spectra whether short H-bonds are formed between water molecules, between the anion and water in the first hydration shell, or a combination of both.[43] Here a small enhancement of the tetrahedrality of water in the second hydration shell of F^- has been observed (at low concentrations),[53] and a local contraction of r_{O4}, r_{OH2}, and r_{HO1}, in particular in the first hydration shell, indicating stronger water−water H-bonds between water molecules in the first and second

dx.doi.org/10.1021/jp309312q | J. Phys. Chem. B 2013, 117, 589−601

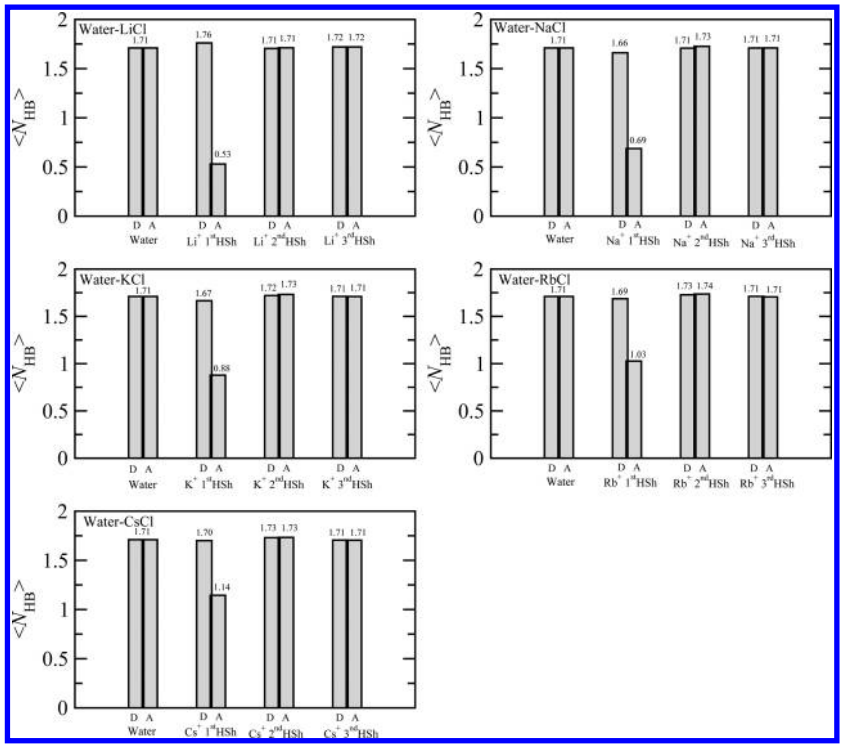

Figure 8. Average number of donor (D) and acceptor (A) H-bonds for neat water and at the first, second, and third hydration shells of the alkali cations.

Table 2. H-Bond Lifetimes for Water in the First, Second, and Third Hydration Shells of the Alkali Cations and Halide Anions[a]

	τ_{HB} (ps), 1st HSh		τ_{HB} (ps), 2nd HSh		τ_{HB} (ps), 3rd HSh	
	D[b]	A[c]	D	A	D	A
water[d]	0.16	0.15	0.17	0.17	0.17	0.17
Li^+	0.21	0.12	0.16	0.17	0.17	0.17
Na^+	0.16	0.12	0.16	0.16	0.17	0.17
K^+	0.15	0.14	0.17	0.16	0.17	0.17
Rb^+	0.16	0.15	0.17	0.16	0.17	0.17
Cs^+	0.16	0.16	0.17	0.16	0.17	0.17
F^-	0.16	0.20	0.18	0.17	0.17	0.17
Cl^-	0.14	0.17	0.17	0.17	0.17	0.17
Br^-	0.15	0.16	0.17	0.17	0.17	0.18
I^-	0.16	0.17	0.17	0.16	0.18	0.18

[a]For pure water at 298 K, a single water molecule was taken as the solute and τ_{HB} was calculated for the first, second, and third self-hydration shells. [b]Donor H-bonds. [c]Acceptor H-bonds. [d]The H-bond lifetime of pure water at 298 K calculated for all the water molecules is 0.20 ps.

hydration shell. Nevertheless, the low tetrahedral enhancement of water in F^-'s second hydration shell and the contraction of these local structural parameters also hints at a larger local density of water around F^-, although not equivalent to either water at low T or high P (see Figure 6b), in apparent contradiction to the interpretation of XAS results, in terms of HDL and LDL water, associated respectively with distorted and tetrahedral H-bond structures.[42,116] Thus, although AMOEBA water is more tetrahedral around F^-, it is not nearly like supercooled water or ice.[53] We have not probed here, however, the tetrahedrality of water in the first hydration shell, where a vertex (O atom) has been replaced by F^-. On the other hand, it should be noted that, among the systems studied, NaF is the only salt that induces a volume contraction,[53] relative to water at 1 atm and 298.15 K; AMOEBA F^- has the smallest first hydration shell among alkali and halide ions and smaller than neat water (O−O), and a CN of 5.9 (O atoms) at 0.2 M, larger than the recent neutron diffraction value of 5.0 reported by Mason et al.[119] The AMOEBA average F^-−O distance from the first peak maximum of the respective rdf is 2.77 Å, slightly lower than the AMOEBA O−O rdf distance, 2.81 Å, in neat water,[53] and larger than most experimental and MD values, 2.6−2.7 Å.[7,65,81]

Figure 10 and Table 2 show that F^- increases the number and lifetime of acceptor H-bonds in the first hydration shell. For the larger halides, a smaller number of acceptor H-bonds and slightly larger lifetimes are observed. However, if the four (Li^+'s CN) nearest water molecules to the halide anions are considered, instead of the complete first hydration shell, a larger number of H-bonds is observed for F^- (1.77), Cl^-(1.74), Br^-(1.73), and I^-(1.71) but not for the larger alkali cations, for a similar subset of water molecules. Another striking difference between F^- and Li^+ is the fact that the τ_{HB} of donor H-bonds for F^- is not significantly affected. This indicates that water molecules in direct interaction with F^- are still able to act as single water proton donors, N_{HB}^{D} = 0.86 ≅ 1.71/2, while water molecules near Li^+ lose much of their ability to act as single proton acceptors, N_{HB}^{A} = 0.53 < 1.71/2, and any acceptor H-bond formed will break very fast, τ_{HB}^{A} = 0.12 ps. For the largest cations (K^+, Rb^+, and Cs^+) and anions (Cl^-, Br^-, and I^-) not all the water molecules in the first hydration shell are in direct interaction with the cation or anion, which means that water molecules at the outer edge of the first peak of the X^+−O and Y^-−O rdf's are free to accept and donate two H-bonds, respectively. This is the reason for N_{HB}^{A} and N_{HB}^{D} in the first hydration shell of these cations and anions, respectively, to be

dx.doi.org/10.1021/jp309312q | J. Phys. Chem. B 2013, 117, 589−601

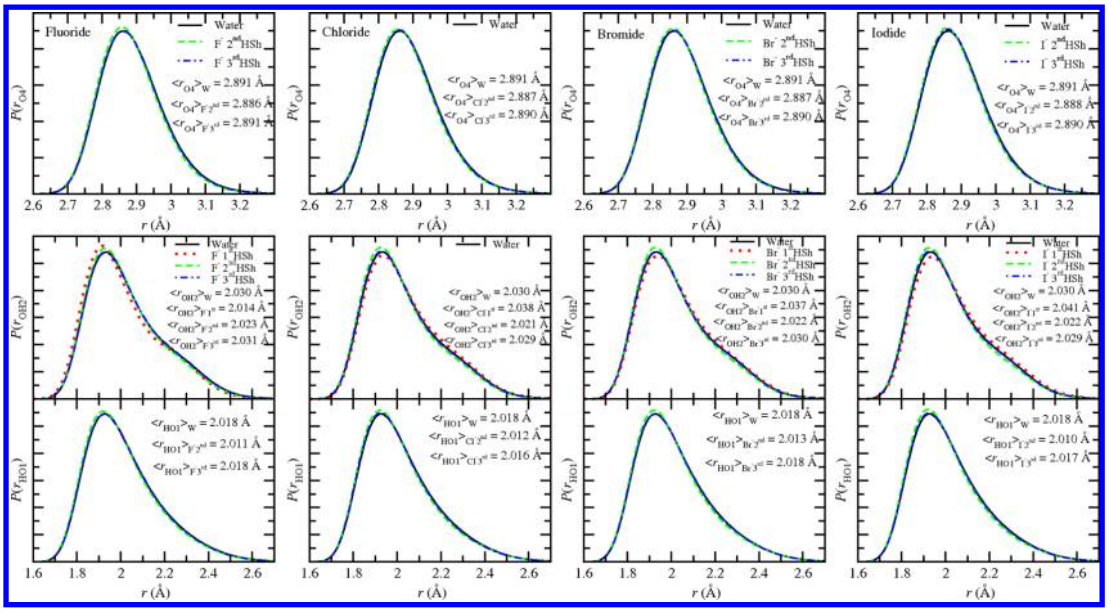

Figure 9. Structure parameters, r_{O4}, r_{OH2}, and r_{HO1}, distribution for the first (r_{OH2}), second, and third hydration shells of the halide anions. The respective average values are given in the plots.

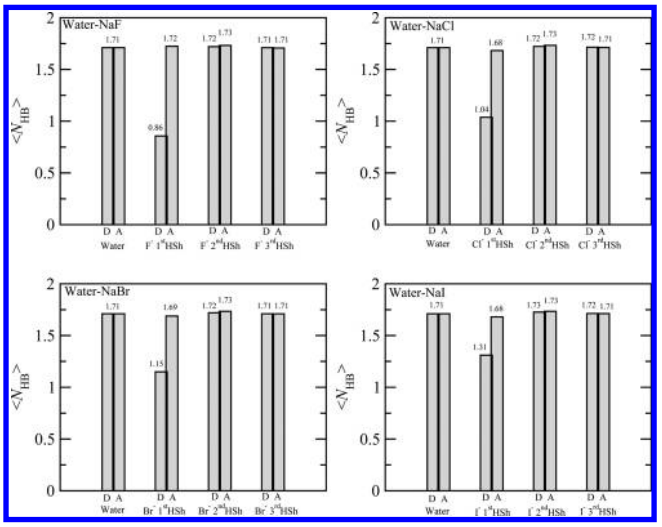

Figure 10. Average number of donor (D) and acceptor (A) H-bonds for neat water and at the first, second, and third hydration shells of the halide anions.

larger than half of the number of H-bonds (~1.71) in liquid water (see Figures 8 and 10).

Ionic Mobility. Theories of ionic mobility[120−131] have long been proposed to explain ion mobility at infinite dilution, in particular the abnormal increase of ionic mobility, with ionic size, for alkali and halide ions, opposite to the Stokes law.[120] The solventberg model substitutes the ionic radius by an "effective" Stokes radius, defined by the radius of the solvated ion, the latter decreasing with increasing ionic radius. Thus, in this model, ions tightly bound to water, like Li^+, diffuse through the solvent with their hydration shell intact. For large, weakly hydrated ions, the solventberg model requires the definition of a number of water molecules that diffuse with the ion, necessarily smaller than the static coordination number.[61] Thus, the solventberg model provides a physically most satisfactory explanation on the mobility of small strongly hydrated ions (kosmotropes). The continuum dielectric friction model[121−125] puts forward a completely different explanation, based on the concept of dielectric friction that results from dielectric relaxation of the solvent, in response to the motion of the polarizing ions. This additional (dielectric) friction decreases with increasing ionic radius, as opposed to the hydrodynamic friction from the Stokes law. Molecular theories[126−131] have also been proposed, based on a splitting of the ion−solvent forces, in short-range repulsive and long-range attractive components. The ionic friction defined in terms of the self-correlation function of the random force acting on the ion is then given in terms of repulsive and attractive force, self-and cross-correlation functions.[64,65] A generalization of this theory, originally proposed by Wolynes,[126,127,131] was given by Byswas and Bagchi,[128−130] and good agreement was found for the mobility of alkali cations in water.[130] Impey et al.[61] proposed a distinct model based on a friction coefficient defined in terms of a nonuniform viscosity, $\eta(r)$. Another MD study[64] focused on the calculation of the ionic friction coefficients for different

Table 3. Ionic Radii, r_{ion}, of the AMOEBA Force Field, Ionic Self-Diffusion Coefficients, D, and Ionic Mobility, u_q

	cations				anions		
	r_{ion} (Å)	D_+ (10^{-5} cm^2/s)	u_q^+ (10^{-4} cm^2/Vs)		r_{ion} (Å)	D_- (10^{-5} cm^2/s)	u_q^- (10^{-4} cm^2/Vs)
Li^+	1.19	0.78 ± 0.05	3.04 ± 0.2	F^-	1.70	1.05 ± 0.05	4.09 ± 0.2
Na^+	1.51	1.09 ± 0.06	4.24 ± 0.2	Cl^-	2.07	1.33 ± 0.05	5.18 ± 0.2
K^+	1.86	1.33 ± 0.06	5.18 ± 0.2	Br^-	2.19	1.38 ± 0.06	5.37 ± 0.2
Rb^+	2.07	1.59 ± 0.07	6.19 ± 0.3	I^-	2.33	1.26 ± 0.05	4.91 ± 0.2
Cs^+	2.19	1.50 ± 0.05	5.84 ± 0.2				

dx.doi.org/10.1021/jp309312q | J. Phys. Chem. B 2013, 117, 589−601

separations of the random force correlation function, and concluded that none of the existent theories explains both positive and negative ion mobilities, in hydrogen-bonded solvents such as water. Even though the calculation of the ionic friction coefficients is outside the scope of the present work, we have calculated the self-diffusion coefficient of the ions to probe the ionic mobility of the AMOEBA cations and anions. In particular, we are interested in the possible structural distinct responses of water near different ions that accompanies ion−water (small ions) and water−ion (large ions) polarization and subsequent dielectric relaxation, at the origin of dielectric friction. The self-diffusion coefficients and respective mobilities for the AMOEBA ions are reported in Table 3. As it may be seen, u_q increases from Li^+ to Rb^+ and from F^- to Br^- and it decreases for Cs^+ and I^-, respectively, in agreement with experiments and previous MD simulations on the mobility of alkali halides in water,[65,67,68] although lower u_q are found for the AMOEBA ions. The most notorious difference between our results and those of Koneshan et al.,[65] for the SPC/E model of water, concern the difference between the relative mobility of Li^+ and F^-, in that we find a lower mobility for Li^+, in qualitative agreement with experimental data.[61,65] Thus, ionic mobility is consistent with the formation of high density H-bonded water cages around small ions, observed in the present work, explaining the exceptionally low entropy of hydration and mobility of Li^+ and F^- and the reciprocal lower mobility and entropy of water molecules in the vicinity of these ions. For K^+, Rb^+, and Cs^+ and for Cl^- and Br^-, a significantly larger mobility is observed, consistent with the observed expansion of the H-bond network of water in the first hydration shell of these ions, although the larger mobility of Rb^+ and Br^-, relative to K^+ and Cl^-, respectively, does not reflect in some of the probed structural perturbations of water. Thus, a lower expansion of water, a larger number of H-bonds and longer H-bond lifetimes are observed for water molecules around Rb^+, relative to K^+. The situation is much similar for Br^- and Cl^-. A significant structural difference exists, however, between these ions, specifically, the fact that K^+ induces a larger disruption of the tetrahedrality of water than Rb^+ and Br^- induces a lower enhancement[53] than Cl^-. Furthermore, the larger mobility of cations relative to anions also correlates well with the opposite effect of cations and anions on the water tetrahedrality in the second hydration shell. The relatively low mobility of I^-, in opposition to Cs^+, is also consistent with the enhanced tetrahedrality[53] of the H-bond network around I^-. This behavior suggests that both anion tetrahedrality enhancement induction and cation induced tetrahedrality disruption are related to the ionic friction increase. Nevertheless, a larger dielectric friction should be associated to more tetrahedral water, explaining the lower mobility of halide anions relative to alkali cations of similar size. Thus, assuming that either water tetrahedrality enhancement or disruption are associated to increased ionic friction, larger mobility is expected for those ions for which the orientational order of surrounding water is least perturbed relative to neat or bulk water. This is in fact observed as Rb^+ and Cs^+ have significantly larger mobilities than the other alkali cations and the halide anions, and a second hydration shell similar to neat water, regarding water tetrahedrality. In relation to Na^+, the self-diffusion coefficient, $D_{Na^+} = 1.09 \times 10^{-5}$ cm^2 s^{-1}, is only marginally larger than that of F^-, $D_{F^-} = 1.05 \times 10^{-5}$ cm^2 s^{-1}, even though the H-bond network of water expands in the first hydration shell of Na^+ and it compresses around F^-. However, Na^+ induces the largest tetrahedrality disruption among the alkali cations. The experimental mobility of Na^+ is actually lower than that of F^- according to the data presented by Koneshan et al.,[65] but in disagreement with both MD[61,65] and the experimental self-diffusion coefficients reported in the article of Impey et al.[61] from Robinson and Stokes,[132] $D_{F^-} = 0.86 \times 10^{-5}$ cm^2 s^{-1} and $D_{Na^+} = 0.91 \times 10^{-5}$ cm^2 s^{-1} at 278 and 282 K, respectively. These data are consistent with the AMOEBA self-diffusion coefficients and support to some extent the weak kosmotrope borderline reputation of Na^+, in that it displays some local hydration characteristics of a chaotrope and mobility similar to that of F^-, a strong kosmotrope.

IV. CONCLUDING REMARKS

The local structure and H-bond lifetime of water in the hydration shells of sodium halide and alkali chloride ∼0.2 M aqueous solutions were studied through MD and compared to those of neat water at different T and P. A significant electrostriction is observed in the first hydration shell of Li^+ and F^-. For the larger alkali cations and halide anions, a small expansion of water in the first ionic hydration shell is observed instead. A fundamental difference between cationic and anionic hydration concerns the orientational order of water in the second ionic hydration shell, in that small alkali cations, in particular, Li^+, Na^+, and K^+, disrupt the tetrahedrality of water and the halide anions enhance the H-bond network tetrahedrality.

The present results indicate that the exceptionally large negative entropy of hydration of small ions like Li^+ and F^-, which bind tightly to water, is also associated to strong electrostriction effects in the first hydration shell, inexistent for larger ions, characterized by milder negative entropies of hydration. Furthermore, electrostriction of water in the first ionic hydration shell explains the lower mobility and entropy of water molecules around small high charge density ions, relative to bulk water. The lower entropy of water molecules around halide anions relative to iso-electronic alkali cations also correlates well with the observed tetrahedrality enhancement of the H-bond network in the second ionic hydration shell of anions. Moreover, the larger mobility of cations relative to anions, of similar size, observed experimentally, also appears to be related with the opposite effects of cations and anions on the local tetrahedrality of water. Finally, the tetrahedrality of water in the second hydration shell of large ions like Cs^+ and I^- suggests that for large ions, independent of their charge, volume exclusion effects associated to cavity formation promote the tetrahedrality of water, similar to the hydration of hydrophobic solutes.

AUTHOR INFORMATION

Corresponding Author

*E-mail: ngalamba@cii.fc.ul.pt.

Notes

The authors declare no competing financial interest.

ACKNOWLEDGMENTS

The author gratefully acknowledges financial support from Fundação para a Ciência e a Tecnologia from Portugal through the project PTDC/QUI-QUI/113376/2009.

REFERENCES

(1) Bernal, J. D.; Fowler, R. H. *J. Chem. Phys.* **1933**, *1*, 515.

(2) Cox, W. M.; Wolfenden, J. H. *Proc. R. Soc. London, Ser. A* **1934**, *145*, 475.
(3) Frank, H. S.; Evans, M. W. *J. Chem. Phys.* **1945**, *13*, 507.
(4) Frank, H. S.; Wen, W. Y. *Discuss. Faraday Soc.* **1957**, 133.
(5) Bakker, H. J. *Chem. Rev.* **2008**, *108*, 1456.
(6) Marcus, Y. *Chem. Rev.* **2009**, *109*, 1346.
(7) Ohtaki, H.; Radnai, T. *Chem. Rev.* **1993**, *93*, 1157.
(8) Samoilov, O. Y. *Discuss. Faraday Soc.* **1957**, 141.
(9) Collins, K. D.; Washabaugh, M. W. *Q. Rev. Biophys.* **1985**, *18*, 323.
(10) Zhang, Y.; Cremer, P. S. *Curr. Opin. Chem. Biol.* **2006**, *10*, 658.
(11) Baldwin, R. L. *Biophys. J.* **1996**, *71*, 2056.
(12) Jungwirth, P.; Winter, B. *Annu. Rev. Phys. Chem.* **2008**, *59*, 343.
(13) Kunz, W.; Lo Nostro, P.; Ninham, B. W. *Curr. Opin. Colloid Interface Sci.* **2004**, *9*, 1.
(14) Jungwirth, P.; Tobias, D. J. *Chem. Rev.* **2006**, *106*, 1259.
(15) Collins, K. D. *Biophys. Chem.* **2012**, *167*, 43.
(16) Bakker, H. J.; Kropman, M. F.; Omta, A. W. *J. Phys.: Condens. Matter* **2005**, *17*, S3215.
(17) Bouazizi, S.; Nasr, S. *J. Mol. Liq.* **2011**, *162*, 78.
(18) Buchner, R.; Chen, T.; Hefter, G. *J. Phys. Chem. B* **2004**, *108*, 2365.
(19) Cappa, C. D.; Smith, J. D.; Messer, B. M.; Cohen, R. C.; Saykally, R. J. *J. Phys. Chem. B* **2006**, *110*, 5301.
(20) Collins, K. D. *Proc. Natl. Acad. Sci. U.S.A.* **1995**, *92*, 5553.
(21) Collins, K. D.; Neilson, G. W.; Enderby, J. E. *Biophys. Chem.* **2007**, *128*, 95.
(22) Corridoni, T.; Mancinelli, R.; Ricci, M. A.; Bruni, F. *J. Phys. Chem. B* **2011**, *115*, 14008.
(23) Fayer, M. D.; Moilanen, D. E.; Wong, D.; Rosenfeld, D. E.; Fenn, E. E.; Park, S. *Acc. Chem. Res.* **2009**, *42*, 1210.
(24) Kropman, M. F.; Bakker, H. J. *Science* **2001**, *291*, 2118.
(25) Kropman, M. F.; Bakker, H. J. *J. Chem. Phys.* **2001**, *115*, 8942.
(26) Kropman, M. F.; Bakker, H. J. *J. Am. Chem. Soc.* **2004**, *126*, 9135.
(27) Kropman, M. F.; Nienhuys, H.-K.; Bakker, H. J. *Phys. Rev. Lett.* **2002**, *88*, 077601.
(28) Leberman, R.; Soper, A. K. *Nature* **1995**, *378*, 364.
(29) Mancinelli, R.; Botti, A.; Bruni, F.; Ricci, M. A.; Soper, A. K. *Phys. Chem. Chem. Phys.* **2007**, *9*, 2959.
(30) Mancinelli, R.; Botti, A.; Bruni, F.; Ricci, M. A.; Sopper, A. K. *J. Phys. Chem. B* **2007**, *111*, 13570.
(31) Omta, A. W.; Kropman, M. F.; Woutersen, S.; Bakker, H. J. *Science* **2003**, *301*, 347.
(32) Omta, A. W.; Kropman, M. F.; Woutersen, S.; Bakker, H. J. *J. Chem. Phys.* **2003**, *119*, 12457.
(33) Perera, P. N.; Browder, B.; Ben-Amotz, D. *J. Phys. Chem. B* **2009**, *113*, 1805.
(34) Smith, J. D.; Saykally, R. J.; Geissler, P. L. *J. Am. Chem. Soc.* **2007**, *129*, 13847.
(35) Soper, A. K.; Weckstrom, K. *Biophys. Chem.* **2006**, *124*, 180.
(36) Tielrooij, K. J.; Garcia-Araez, N.; Bonn, M.; Bakker, H. J. *Science* **2010**, *328*, 1006.
(37) Tielrooij, K. J.; van der Post, S. T.; Hunger, J.; Bonn, M.; Bakker, H. J. *J. Phys. Chem. B* **2011**, *115*, 12638.
(38) Turton, D. A.; Hunger, J.; Hefter, G.; Buchner, R.; Wynne, K. *J. Chem. Phys.* **2008**, 128.
(39) van der Post, S. T.; Bakker, H. J. *Phys. Chem. Chem. Phys.* **2012**, *14*, 6280.
(40) Westh, P.; Kato, H.; Nishikawa, K.; Koga, Y. *J. Phys. Chem. A* **2006**, *110*, 2072.
(41) Mile, V.; Gereben, O.; Kohara, S.; Pusztai, L. *J. Phys. Chem. B* **2012**, *116*, 9758.
(42) Waluyo, I.; Huang, C.; Nordlund, D.; Bergmann, U.; Weiss, T. M.; Pettersson, L. G. M.; Nilsson, A. *J. Chem. Phys.* **2011**, *134*, 064513.
(43) Waluyo, I.; Huang, C. C.; Nordlund, D.; Weiss, T. M.; Pettersson, L. G. M.; Nilsson, A. *J. Chem. Phys.* **2011**, *134*, 224507.
(44) Lin, Y. S.; Auer, B. M.; Skinner, J. L. *J. Chem. Phys.* **2009**, *131*, 144511.
(45) Boisson, J.; Stirnemann, G.; Laage, D.; Hynes, J. T. *Phys. Chem. Chem. Phys.* **2011**, *13*, 19895.
(46) Carrillo-Tripp, M.; Saint-Martin, H.; Ortega-Blake, I. *J. Chem. Phys.* **2003**, *118*, 7062.
(47) Chandra, A. *Phys. Rev. Lett.* **2000**, *85*, 768.
(48) Chandra, A.; Chowdhuri, S. *J. Phys. Chem. B* **2002**, *106*, 6779.
(49) Chandrasekhar, J.; Jorgensen, W. L. *J. Chem. Phys.* **1982**, *77*, 5080.
(50) Chandrasekhar, J.; Spellmeyer, D. C.; Jorgensen, W. L. *J. Am. Chem. Soc.* **1984**, *106*, 903.
(51) Chialvo, A. A.; Simonson, J. M. *J. Mol. Liq.* **2004**, *112*, 99.
(52) Corradini, D.; Rovere, M.; Gallo, P. *J. Phys. Chem. B* **2011**, *115*, 1461.
(53) Galamba, N. *J. Phys. Chem. B* **2012**, *116*, 5242.
(54) Galamba, N.; Cabral, B. J. C. *J. Phys. Chem. B* **2009**, *113*, 16151.
(55) Gallo, P.; Corradini, D.; Rovere, M. *Phys. Chem. Chem. Phys.* **2011**, *13*, 19814.
(56) Grossfield, A.; Ren, P. Y.; Ponder, J. W. *J. Am. Chem. Soc.* **2003**, *125*, 15671.
(57) Guardia, E.; Marti, J.; Garcia-Tarres, L.; Laria, D. *J. Mol. Liq.* **2005**, *117*, 63.
(58) Holzmann, J.; Ludwig, R.; Geiger, A.; Paschek, D. *Angew. Chem., Int. Ed.* **2007**, *46*, 8907.
(59) Hribar, B.; Southall, N. T.; Vlachy, V.; Dill, K. A. *J. Am. Chem. Soc.* **2002**, *124*, 12302.
(60) Ikeda, T.; Boero, M.; Terakura, K. *J. Chem. Phys.* **2007**, *126*, 034501.
(61) Impey, R. W.; Madden, P. A.; McDonald, I. R. *J. Phys. Chem.* **1983**, *87*, 5071.
(62) Irudayam, S. J.; Henchman, R. H. *J. Chem. Phys.* **2012**, *137*, 034508.
(63) Kim, J. S.; Yethiraj, A. *J. Phys. Chem. B* **2008**, *112*, 1729.
(64) Koneshan, S.; Lynden-Bell, R. M.; Rasaiah, J. C. *J. Am. Chem. Soc.* **1998**, *120*, 12041.
(65) Koneshan, S.; Rasaiah, J. C.; Lynden-Bell, R. M.; Lee, S. H. *J. Phys. Chem. B* **1998**, *102*, 4193.
(66) Laage, D.; Hynes, J. T. *Proc. Natl. Acad. Sci. U.S.A.* **2007**, *104*, 11167.
(67) Lee, S. H.; Rasaiah, J. C. *J. Chem. Phys.* **1994**, *101*, 6964.
(68) Lee, S. H.; Rasaiah, J. C. *J. Phys. Chem.* **1996**, *100*, 1420.
(69) Lightstone, F. C.; Schwegler, E.; Hood, R. Q.; Gygi, F.; Galli, G. *Chem. Phys. Lett.* **2001**, *343*, 549.
(70) Lynden-Bell, R. M.; Rasaiah, J. C. *J. Chem. Phys.* **1997**, *107*, 1981.
(71) Lyubartsev, A. P.; Laasonen, K.; Laaksonen, A. *J. Chem. Phys.* **2001**, *114*, 3120.
(72) Sala, J.; Guardia, E.; Marti, J. *J. Chem. Phys.* **2010**, 132.
(73) Suresh, S. J.; Kapoor, K.; Talwar, S.; Rastogi, A. *J. Mol. Liq.* **2012**, *174*, 135.
(74) Tongraar, A.; Liedl, K. R.; Rode, B. M. *J. Phys. Chem. A* **1997**, *101*, 6299.
(75) Tongraar, A.; Liedl, K. R.; Rode, B. M. *J. Phys. Chem. A* **1998**, *102*, 10340.
(76) Topol, I. A.; Tawa, G. J.; Burt, S. K.; Rashin, A. A. *J. Chem. Phys.* **1999**, *111*, 10998.
(77) White, J. A.; Schwegler, E.; Galli, G.; Gygi, F. *J. Chem. Phys.* **2000**, *113*, 50435.
(78) Zhu, S. B.; Robinson, G. W. *J. Chem. Phys.* **1992**, *97*, 4336.
(79) Chowdhuri, S.; Chandra, A. *J. Phys. Chem. B* **2006**, *110*, 9674.
(80) Chowdhuri, S.; Chandra, A. *Phys. Rev. E* **2002**, 66.
(81) Heuft, J. M.; Meijer, E. J. *J. Chem. Phys.* **2005**, *122*, 7.
(82) Jenkins, H. D. B.; Pritchett, M. S. F. *J. Chem. Soc., Faraday Trans. 1* **1984**, *80*, 721.
(83) Marcus, Y. *J. Chem. Soc., Faraday Trans.* **1991**, *87*, 2995.
(84) Marcus, Y.; Loewenschuss, A. *Annu. Rep. Prog. Chem., Sect. C: Phys. Chem.* **1984**, *81*, 81.
(85) Graziano, G. *Chem. Phys. Lett.* **2009**, *479*, 56.
(86) Hofmeister, F. *Arch. Exp. Pathol. Pharmakol.* **1888**, *24*, 247.
(87) Tobias, D. J.; Hemminger, J. C. *Science* **2008**, *319*, 1197.

(88) Desnoyer, J. E.; Verrall, R. E.; Conway, B. E. *J. Chem. Phys.* **1965**, *43*, 243.
(89) Drude, P.; Nernst, W. *Z. Phys. Chem.* **1894**, *15*, 79.
(90) Marcus, Y. *J. Phys. Chem. B* **2005**, *109*, 18541.
(91) Marcus, Y. *Chem. Rev.* **2012**, *111*, 2761.
(92) Marcus, Y.; Hefter, G. *J. Solution Chem.* **1999**, *28*, 575.
(93) Webb, T. J. *J. Am. Chem. Soc.* **1926**, *48*, 2589.
(94) Ren, P. Y.; Ponder, J. W. *J. Comput. Chem.* **2002**, *23*, 1497.
(95) Ren, P. Y.; Ponder, J. W. *J. Phys. Chem. B* **2003**, *107*, 5933.
(96) Halgren, T. A. *J. Am. Chem. Soc.* **1992**, *114*, 7827.
(97) Ponder, J. W. *TINKER: Software Tools for Molecular Design, 5.1*; Washington University School of Medicine: Saint Louis, MO, 2010.
(98) Berendsen, H. J. C.; Postma, J. P. M.; Vangunsteren, W. F.; Dinola, A.; Haak, J. R. *J. Chem. Phys.* **1984**, *81*, 3684.
(99) Chau, P. L.; Hardwick, A. J. *Mol. Phys.* **1998**, *93*, 511.
(100) Errington, J. R.; Debenedetti, P. G. *Nature* **2001**, *409*, 318.
(101) Starr, F. W.; Nielsen, J. K.; Stanley, H. E. *Phys. Rev. Lett.* **1999**, *82*, 2294.
(102) Haile, J. M. *Molecular Dynamics Simulation: Elementary Methods*; Wiley Professional: New York, 1997.
(103) Chen, S.-H.; Teixeira, J. *Adv. Chem. Phys.* **1986**, 64.
(104) Conde, O.; Teixeira, J. *J. Phys. (Paris)* **1983**, *44*, 525.
(105) Conde, O.; Teixeira, J. *Mol. Phys.* **1984**, *53*, 951.
(106) Montrose, C. J.; Bucaro, J. A.; Marshall., J.; Litovitz, T. A. *J. Chem. Phys.* **1974**, *60*, 5025.
(107) Starr, F. W.; Nielsen, J. K.; Stanley, H. E. *Phys. Rev. E* **2000**, *62*, 579.
(108) Paesani, F.; Voth, G. A. *J. Phys. Chem. B* **2009**, *113*, 5702.
(109) Ren, P. Y.; Ponder, J. W. *J. Phys. Chem. B* **2004**, *108*, 13427.
(110) Mills, R. *J. Phys. Chem.* **1973**, *77*, 685.
(111) Enderby, J. E. *Chem. Soc. Rev.* **1995**, *24*, 159.
(112) Enderby, J. E.; Neilson, G. W. *Rep. Prog. Phys.* **1981**, *44*, 593.
(113) Neilson, G. W.; Mason, P. E.; Ramos, S.; Sullivan, D. *Philos. Trans. R. Soc., A* **2001**, *359*, 1575.
(114) Newsome, J. R.; Neilson, G. W.; Enderby, J. E. *J. Phys. C: Solid State Phys.* **1980**, *13*, L923.
(115) Rempe, S. B.; Pratt, L. R.; Hummer, G.; Kress, J. D.; Martin, R. L.; Redondo, A. *J. Am. Chem. Soc.* **2000**, *122*, 966.
(116) Huang, C.; Wikfeldt, K. T.; Tokushima, T.; Nordlund, D.; Harada, Y.; Bergmann, U.; Niebuhr, M.; Weiss, T. M.; Horikawa, Y.; Leetmaa, M.; Ljungberg, M. P.; Takahashi, O.; Lenz, A.; Ojamäe, L.; Lyubartsev, A. P.; Shin, S.; Pettersson, L. G. M.; Nilsson, A. *Proc. Natl. Acad. Sci. U.S.A.* **2009**, *106*, 15214.
(117) Mateus, M. P. S.; Galamba, N.; Costa Cabral, B. J. *J. Chem. Phys.* **2012**, *136*, 014507.
(118) Laage, D.; Hynes, J. T. *J. Phys. Chem. B* **2008**, *112*, 7697.
(119) Mason, P. E.; Heyda, J.; Fischer, H. E.; Jungwirth, P. *J. Phys. Chem. B* **2010**, *114*, 13853.
(120) Bagchi, B.; Biswas, R. *Acc. Chem. Res.* **1998**, *31*, 181.
(121) Born, M. *Z. Phys.* **1920**, *1*, 221.
(122) Boyd, R. H. *J. Chem. Phys.* **1961**, *35*, 1281.
(123) Fuoss, R. M. *Proc. Natl. Acad. Sci. U.S.A.* **1959**, *45*, 807.
(124) Hubbard, J.; Onsager, L. *J. Chem. Phys.* **1977**, *67*, 4850.
(125) Zwanzig, R. *J. Chem. Phys.* **1963**, *38*, 1603.
(126) Wolynes, P. G. *J. Chem. Phys.* **1978**, *68*, 473.
(127) Wolynes, P. G. *Annu. Rev. Phys. Chem.* **1980**, *31*, 345.
(128) Biswas, R.; Bagchi, B. *J. Am. Chem. Soc.* **1997**, *119*, 5946.
(129) Biswas, R.; Bagchi, B. *J. Chem. Phys.* **1997**, *106*, 5587.
(130) Biswas, R.; Roy, S.; Bagchi, B. *Phys. Rev. Lett.* **1995**, *75*, 1098.
(131) Colonomos, P.; Wolynes, P. G. *J. Chem. Phys.* **1979**, *71*, 2644.
(132) Robinson, R. A.; Stokes, R. H. *Electrolyte Solutions*; Butterworths: London, 1955.